 FDMP, vol.2, no.1, pp.17-26, 2006

Thermocapillary Effects in Systems with Variable Liquid Mass Exposed to Concentrated Heating

M.El-Gammal[1] **and J.M.Floryan**[1]

Abstract: Interface deformation and thermocapillary rupture in a cavity with free upper surface subject to concentrated heating from above is investigated. The dynamics of the process is modulated by placing different amounts of liquid in the cavity. The results determined for large Biot and zero Marangoni numbers show the existence of limit points beyond which steady, continuous interface cannot exist and processes leading to the interface rupture develop. Evolution of the limit point as a function of the mass of the liquid is investigated. The topology of the flow field is found to be qualitatively similar, regardless of whether the cavity is over-filled or only partially filled. The available results demonstrate that cavity over-filling is an effective strategy for prevention of interface rupture, but only when the flow Reynolds number is small. This strategy becomes completely ineffective for high enough Re and deep enough liquid. Cavity over-filling can thus be used as a tool for prevention of rupture, but only under restrictive range of parameters.

keyword: Interface rupture, Thermocapillary convection, Non-planar interfaces

1 Introduction

Thermocapillary flows are driven by the imbalance of the tangential stress on a liquid free surface caused by temperature dependence of surface tension (Scriven and Sterling, 1960). Thermocapillary effects give rise to various gravity independent phenomena arising at differentially heated free liquid interfaces. These phenomena include convective flows as well as interface distortions, including interface rupture. Convective flows and the associated instabilities have been subjected to numerous investigations (Kuhlmann, 1999; Schatz and Neitzel, 2001; Davis, 1987; Amberg and Shiomi, 2005; Gelfgat et al., 2005; Lappa, 2005a, b) while the analysis of interface deformation and possible rupture has attracted attention more recently (Floryan and Chen, 1994). Convective flow and interface distortion are important in many technical processes involving non-isothermal fluid interfaces. These effects could be dominant (e.g., zero-gravity containerless materials processing) or could represent a contributing factor (e.g., conventional crystal growth or welding). Control and optimisation of these and other processes critically depend on the complete understanding of liquid response driven by thermocapillary effect. The focus of the present work is on studying thermocapillary rupture and thermocapillary flows in the absence of any body forces, and especially in the absence of gravity.

The mechanics of response of fluid dynamical system depends on the type of heating applied to the interface. In the geometrically simplest case of liquid contained in a rectangular cavity open from above, the heating can be applied either through the bottom, or through the sidewalls, or from above. The response of the system is remarkable different in each of these cases. The simplest case of heating through the bottom involves liquid with initially flat interface resting on an isothermal, flat, solid plate. The resulting temperature field gives rise to the temperature gradient vector that is normal to the interface at the interface. The liquid motion can be induced through an instability process first studied by Pearson (1958) when the critical conditions are met. This process is usually referred to as the Marangoni instability. There are two instability mechanisms possible. The first one relies on convective effects and Pearson (1958) determined the relevant critical conditions. The second one relies on the interface deformation and the relevant critical conditions have been established by Czechowski and Floryan (2001). When the cavity is sufficiently long, the second mechanism dominates resulting in an unconditional instability that initiates process leading to the rupture of the interface (Floryan and Chen, 1994).

When the liquid is heated through the sidewalls, such as in the case of horizontal direct crystallization (Berdnikov, Gaponov and Kovrizhnykh, 2001) the resulting

[1] Department of Mechanical and Materials Engineering, The University of Western Ontario, London, Ontario, N5A 5B9, Canada

temperature gradient has a component in the direction parallel to the interface. In this case, the thermocapillary effect always generates some motion, regardless of the magnitude of temperature gradient. Floryan and Chen (1994) showed that a long continuous liquid layer exposed to such heating may exist only when the temperature field satisfies restrictive existence conditions. Chen and Hwu (1993) included effects of interface deformability and concluded that instability may occur at a Marangoni number considerably lower than the one found in the case of a non-deformable interface. Hamed and Floryan (2000a) showed that large interfacial deformations might occur, leading to rupture of the interface through formation of dry spots at the sidewalls if the contact points are fixed. Jiang, Badr and Floryan (2003) demonstrated similar phenomena in the case of fixed contact angles constraint, with rupture leading to the formation of dry spots at the cavity bottom. They determined the location of the limit points in the parameter space beyond which a steady, continuous interface cannot exist (Hamed and Floryan, 2000a; Jiang, Badr and Floryan, 2003). Jiang and Floryan (2003) demonstrated that insulating interface could increase deformation.

When the interface is subject to concentrated heating from above, such as in the case of laser heating, the resulting temperature gradients always generate convection and interface deformation and may lead to interface rupture, as demonstrated by Hamed and Floryan (2000b). Jiang, Badr and Floryan (2003) showed that application of the fixed contact angles rather then fixed contact points conditions significantly increases deformation. Insulating interface could decrease deformation (Jiang and Floryan, 2003). An infinite interface subject to periodic heating may also rupture, as shown by Tan, Bankoff and Davis (1990). Rivas (1991) and Higuera (2000) considered concentrated heat flux applied to the interface but neglected effects of interface deformation. Chen and Lin (2000) considered simulated radiation and included effect of evaporation but did not considered interface deformation. Lee, Kamotani and Yoda (2002) placed electrically heated wire at the interface and identified various flow regimes, including three-dimensional oscillatory states. Pumir and Blumenfeld (1996) considered fixed heat flux and analysed thermocapillary mixing and limits on the maximum possible temperature rise. Herrero and Mancho (1998) studied effects of container aspect ratio on the resulting convection. Feonychev (1995), Nepomnyashchy and Simanovskii (1999) and Simanovskii (2000) considered multiple-layer system assuming non-deformable interfaces.

The present study is focused on the analysis of the dynamics of a liquid system where a certain mass of liquid whose magnitude is constrained only by the isothermal static conditions is placed in a cavity. The permissible forms of the interface are described by the Young-Laplace equation. The temperature gradient along the interface is created by applying concentrated heating from above. Two cases of dynamical response are considered. The first one corresponds to the interface being subject to the fixed contact point constraint and the second one corresponds to the fixed angles constraint. In all cases considered, the initial form of the constraint, i.e., either the initial locations of the contact points or the initial contact angles, is preserved during the heating. El-Gammal, Furmanski and Floryan (2003) considered the case of cavity heated through the sidewalls and suggested that cavity over-filling can be used for control of interface rupture. The present paper investigates this issue in the case of a cavity subject to a concentrated heating at the interface. Since the governing equations are not amenable to analytical solutions under such conditions, we shall rely on numerical simulations.

The paper is organized as follows. Section 2 gives the formulation and explains the notation used. Section 3 is devoted to the discussion of our results. Section 4 gives a short summary of the main conclusions.

2 Problem Formulation

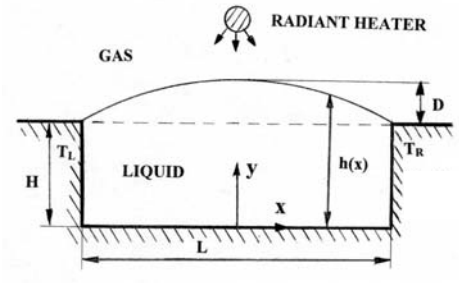

Figure 1 : Sketch of the flow model problem.

Consider liquid in a cavity of length L (Fig. 1) formed by isothermal walls on the left and right sides, by an insulated solid plate on the bottom, and open from above. The liquid is incompressible, Newtonian, has density ρ,

thermal conductivity k, specific heat per unit mass c, thermal diffusivity κ = k / ρ c, kinematic viscosity ν and dynamic viscosity μ. The free surface, described by y = h(x), is bounded by a passive gas of negligible density and viscosity. This free surface is associated with a surface tension σ, which is a function of the local temperature. The cavity is over-filled with the liquid and the shape of the isothermal interface is described by the Laplace-Young equation whose solution in the two-dimensional case in the absence of gravity corresponds to an element of a circle passing through the contact points at (x,y)=($\pm$L/2, H). The initial, isothermal shape of the interface is described as $h_0(x) = D + H + D|D|^{-1}[-R + (R^2 - x^2)^{1/2}]$, where $R = (L^2/4 + D^2)|D|/(2D^2)$ denotes radius of curvature of the interface and D stands for the bulge factor (see Fig.1). The bulge factor D provides a convenient measure of the mass of the liquid; it is positive when the interface bulges out and the cavity is overfilled, and it is negative when the interface bulges in and the cavity is partially filled. When the liquid surface is heated, thermocapillary effect acting along the interface gives rise to two-dimensional steady convection described by the dimensionless field equations in the form

$$u_x + v_y = 0, \tag{1a}$$

$$\mathrm{Re}(uu_x + vu_y) = -p_x + u_{xx} + u_{yy}, \tag{1b}$$

$$\mathrm{Re}(uv_x + vv_y) = -p_y + v_{xx} + v_{yy}, \tag{1c}$$

$$\mathrm{Ma}(uT_x + vT_y) = T_{xx} + T_{yy}. \tag{1d}$$

where p, (u,v) and T denote pressure, velocity vector and temperature, respectively, Re and Ma stand for the Reynolds and Marangoni numbers, respectively, and subscripts denote derivatives. The relevant boundary conditions have the form

$$x = -L/2 : u = v = 0, T = T_L, \tag{2a}$$

$$x = L/2 : u = v = 0, T = T_R, \tag{2b}$$

$$y = 0 : u = v = T_y = 0, \tag{2c}$$

$$y = h(x) : uh_x - v = 0, \tag{2d}$$

$$\begin{aligned} &-p + 2\left[v_y - h_x u_y + h_x(-v_x + h_x u_x)\right](1 + h_x^2)^{-1} \\ &\quad = \mathrm{Ca}^{-1}(1 - \mathrm{CaT})h_{xx}(1 + h_x^2)^{-3/2}, \end{aligned} \tag{2e}$$

$$\begin{aligned} &2h_x(-u_x + v_y) + (1 - h_x^2)(v_x + u_y) \\ &\quad = -(T_x + h_x T_y)(1 + h_x^2)^{1/2}, \end{aligned} \tag{2f}$$

$$(-h_x T_x + T_y)(1 + h_x^2)^{-1/2} + \mathrm{Bi}(T - T_g(x)) = 0 \tag{2g}$$

where Ca and Bi are the capillary and Biot numbers, respectively, $T_g(x)$ describes temperature distribution in the gas phase and h(x) represents location of the interface. The problem is closed by assuming that the total mass of the liquid is conserved and either the contact points or the contact angles remain fixed during the heating, i.e.,

$$\int_{-\frac{1}{2}L}^{\frac{1}{2}L} h(x,t)dx = V. \tag{2h}$$

$$x = \pm L/2 : \text{ either } h = 1 \text{ or } h_x = h_{0x}, \tag{2i}$$

where V is volume of the liquid parameterized by the bulge factor and determined from the conditions of isothermal equilibrium. The assumed gas temperature mimics conditions expected in the case of concentrated heating (e.g., laser heating); this temperature is taken in the Gaussian form following Hamed and Floryan (2000b), i.e., $T_g(x) = 8exp(-x^2)$, and $T_L = T_g(-L/2)$, $T_R = T_g(L/2)$ for consistency of temperature field at the contact points.

Details of scaling and problem formulations can be found in Hamed and Floryan (2000a) and are omitted from this presentation. Since geometrical effects play an important role in this analysis, the reader should note that the elevation of the isothermal contact point plays the role of a length scale, i.e., the length scale is related to the depth of the liquid. The flow problem (1-2) has to be solved on an irregular solution domain whose shape is determined by the unknown location of the free surface h(x). Chen and Floryan (1994) developed the relevant algorithm and its description is omitted from this presentation. Hamed and Floryan (1998) provided extension of this algorithm to time-dependent situations.

3 Discussion of Results

We shall discuss the behaviour of the liquid contained in the cavity shown in Fig. 1. In order to simplify discussion, we shall only consider the conduction limit Ma $\to$ 0

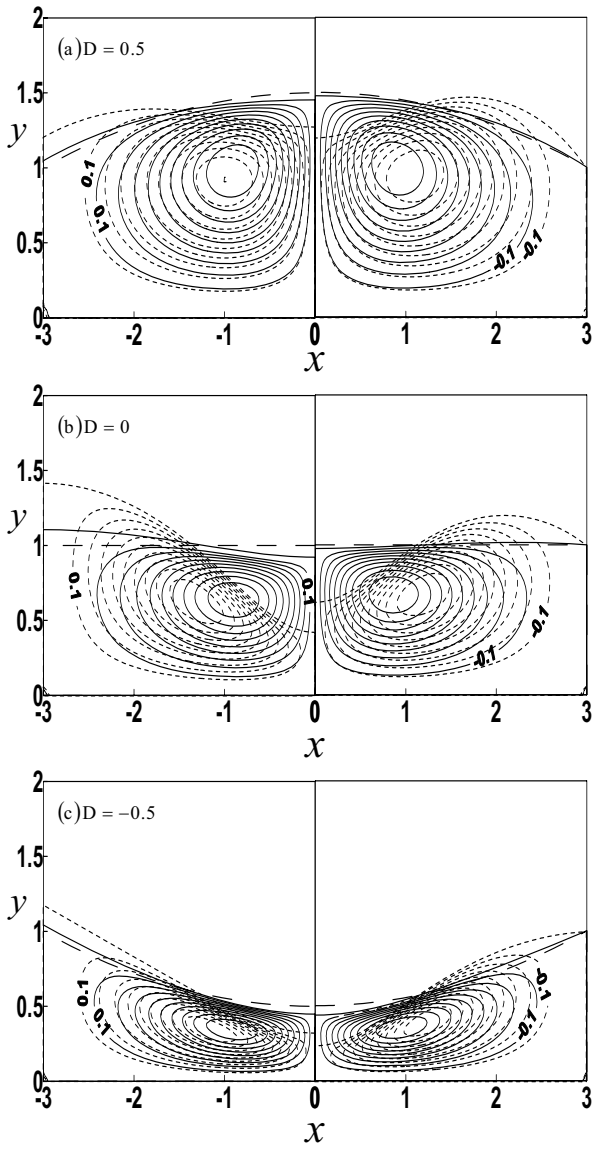

Figure 2 : Flow patterns in a cavity for Re = 1; interface is subject to the fixed contact angles constraint (left side) and the fixed contact points constraint (right side). Contour lines are shown every 10% of ψ_{max}. Long-dash lines show isothermal interface. Figure 2a – D=0.5, left side: solid lines - Ca=0.02, —ψ_{max}—=0.3063; dash lines – Ca=0.07, —ψ_{max}—=0.2807; right side: solid lines - Ca=0.02, —ψ_{max}—=0.3118; dash lines – Ca=0.12, —ψ_{max}—=0.310. Figure 2b – D=0, left side: solid lines - Ca=0.02, —ψ_{max}—=0.1669; dash lines – Ca=0.06, —ψ_{max}—=0.1270; right side: solid lines - Ca=0.01, —ψ_{max}—=0.1809; dash lines – Ca=0.08, —ψ_{max}—=0.1701. Figure 2c – D=-0.5, left side: solid lines - Ca=0.005, —ψ_{max}—=0.0571; dash lines – Ca=0.015, —ψ_{max}—=0.0462; right side: solid lines - Ca=0.01, —ψ_{max}—=0.0583; dash lines – Ca=0.03, —ψ_{max}—=0.0562.

and large Biot number limit Bi $\rightarrow \infty$. The first condition limits our results to highly conductive liquids (k$\rightarrow \infty$) such as liquid metals. The second condition implies a very high heat transfer coefficient in the gas phase at the interface, which makes the temperature of the interface effectively equal to the temperature of the gas phase. We select cavity length L=6 for our discussion as the response of the system with such length with the interface being initially flat is well documented (Hamed and Floryan, 2000b).

3.1 The Fixed Contact Points Case.

Figure 2 illustrates flow patterns in the case of small Reynolds number Re=1 for three values of the bulge parameter, i.e., D=0.5, 0, -0.5. The surface tension is weakest in the cavity centre where the temperature is highest and it drives the liquid away from the centre and towards the sidewalls. Conservation of mass gives rise to longitudinal pressure gradient required to create the backflow along the cavity bottom. The resulting flow pattern has the form of two large, symmetric, re-circulating vortices. The interface recedes in the middle of the cavity and rises around the sidewalls. The centres of the vortices move away from the heating area as the interface deformation increases. Pressure variations illustrated in Fig.3 show that the flow domain might be divided into the central zone with a fairly strong flow and the end zones where the flow is very weak and the pressure is almost constant. The formation of the end zones is associated with the very rapid decreases of the temperature gradient along the interface as one moves away from the heating area. When Ca increases, the magnitude of the deformation increases while preserving its qualitative form. The maximum deformation occurs in the middle of the cavity and its variations as a function of Ca are illustrated in Fig.4. One can clearly see the existence of the limit point beyond which continuous interface cannot exist in each case considered. The shape of the interface suggests eventual formation of a dry spot at the middle of the cavity bottom. The range of the acceptable capillary numbers increases as the mass of the liquid contained in the cavity (as measured by the bulge factor) rises; change of D from D=–0.5 to D=05 more than triples the acceptable values of Ca. Increasing the total mass of the liquid in the cavity represents thus an efficient method for prevention of the rupture under such flow conditions.

Figure 5 illustrates flow patterns for Reynolds number

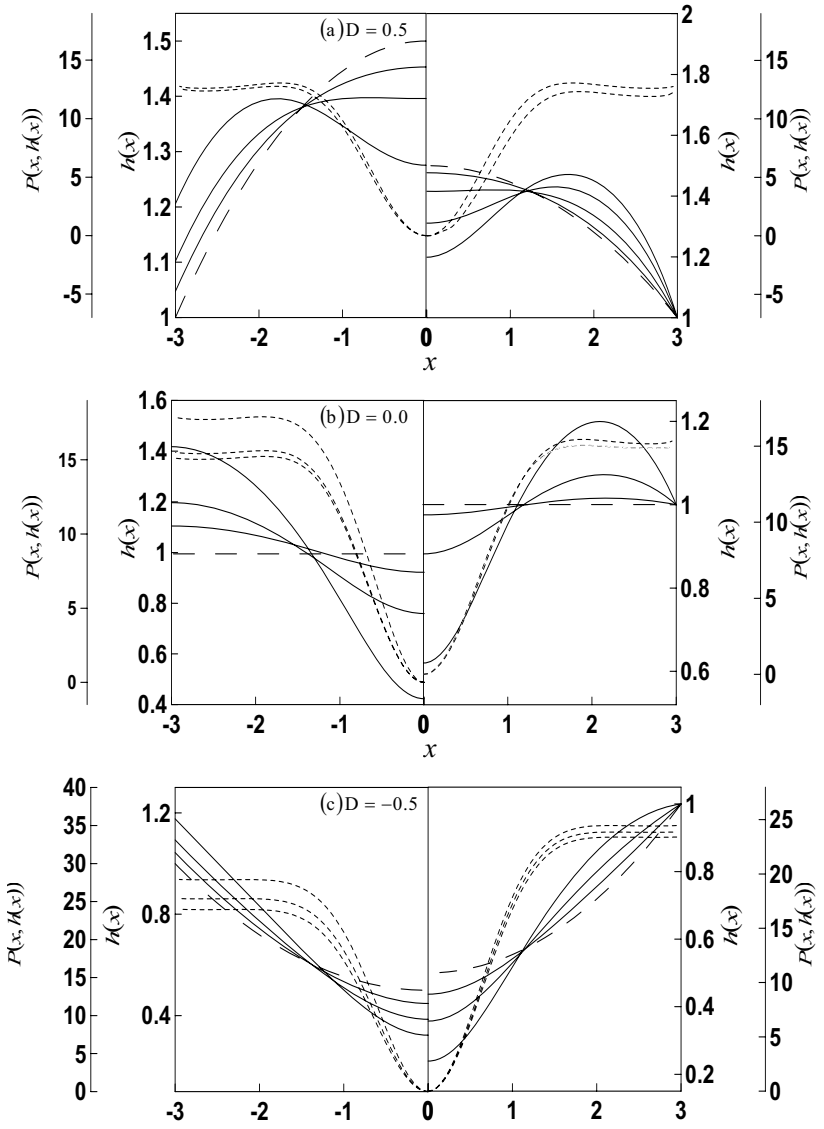

Figure 3 : The evolution of the surface pressure and the shape of the interface as a function of the capillary number Ca for Re=1; the interface subject to the fixed contact angles constraint (left side) and the fixed contact points constraint (right side). The long-dash lines show isothermal interface, solid lines show deformed interface and dash lines show surface pressure. Figure 3a – D=0.5, left side: interface shown for Ca= 0.02, 0.04, 0.07, pressure shown for Ca=0.02, 0.07; right side: interface shown for Ca= 0.02, 0.06, 0.1, 0.12, pressure shown for Ca=0.02, 0.12. Figure 3b – D=0, left side: interface shown for Ca=0.02, 0.04, 0.06; pressure shown for Ca= 0.02, 0.06; right side: interface shown for Ca=0.01, 0.04, 0.08, pressure shown for Ca=0.01, 0.08. Figure 3c –D=-0.5, left side: interface and pressure shown for Ca= 0.005, 0.01, 0.015; right side: interface and pressure shown for Ca=0.01, 0.02, 0.03. The top dash line always corresponds to the pressure with the smallest Ca.

Re=200. In this case centres of the vortices move further towards the sidewalls when compared to the low Reynolds number flow (Fig.2). An additional set of recirculating vortices appears at the cavity bottom directly under the heating area for sufficiently large depth of the liquid. Deformation pattern changes remarkably as compared to the case of Re=1. For large depth of the liquid (D=0.5) the interface rises in the middle of the cavity (Fig.5a) and dips below its isothermal location approximately above the vortex centres. As D decreases, the pat-

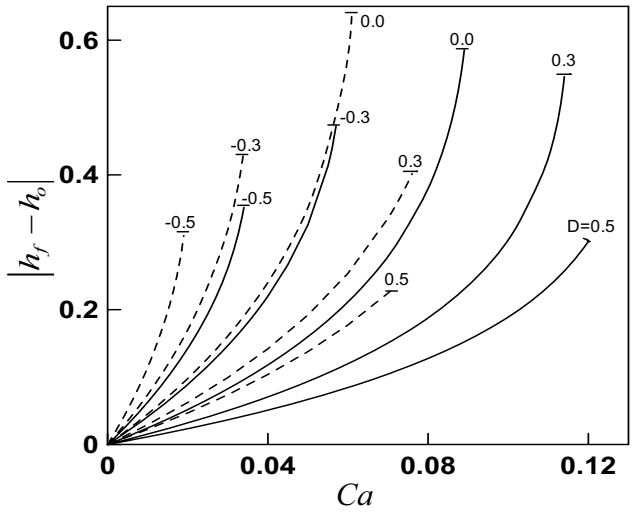

Figure 4 : The interface deformation in the middle of the cavity as a function of the capillary number Ca for different values of the bulge factor D and for Re=1. Continuous and dash lines describe the fixed contact points and the fixed contact angles cases, respectively.

tern eventually reverses itself with the interface receding in the middle and rising around the sidewalls (see Figs5a-c). Pressure variations displayed in Fig.6 demonstrate that significant motion extends over the whole length of the cavity without the near-stagnant liquid in the end zones. Pressure variations are affected by the presence of the vortices, with significant pressure minima located above their centres. The reader may note that the vortices are expected to acquire invicid characteristics as Re increases, however, the depth of the liquid affects their approach towards the inviscid form. Vortex development is little constrained when liquid depth is large (Fig.6a) resulting in large local pressure minima. These minima almost disappear for small liquid depth (Fig.6c) where viscous effects play a relatively larger role. Creation of the second set of vortices and large rise of the interface above its isothermal location in the cavity centre for large cavity depth (Fig.5a) can thus be attributed to the re-arrangement of pressure field associated the vortices acquiring inviscid characteristics.

Variations of the interface deformation in the middle of the cavity as a function of Ca for Re=200 are illustrated in Fig.7. The existence of the limit points is clearly documented for each case considered. There is a remarkable difference, however, in the way the location of the limit point changes as a function of the mass of the liquid. When D<0 the shape of the interface suggest eventual rupture through formation of a dry spot at the cavity bottom; an increase of D from D=-0.5 to D=0 increases Ca_{cr} by approximately a factor of three. When D>0 the shape of the interface suggest eventual rupture through some form of breakdown around the contact points; further increase of D from D=0 to D=0.5 does not change Ca_{cr}. The observed variation of Ca_{cr} as a function of D can be explained by noting that as the depth of the liquid increases, the qualitative properties of the vortices change and the growing inviscid "suction" above vortex centres begins to dominate the interface deformation. Increase of the mass of the liquid, as a method for rupture control, should be considered with caution in this case.

3.2 The Fixed Contact Angles Case

Flow patterns for small Reynolds number Re=1 are illustrated in Fig.2. They are very similar to the patterns observed in the case of fixed contact point constraint discussed above. The deformation is much larger, however, with the interface receding in the cavity centre and rising at the sidewalls. Pressure variations illustrated in Fig.3 demonstrate the existence of regions of nearly stagnant liquid around the cavity sidewalls. The limit point exists in each of the cases considered as illustrated in Fig.4, with its location moving towards the higher values of Ca when the mass of the liquid increases. One may conclude that addition of liquid to the cavity represents a good method for rupture control in this case.

Flow patterns for Re=200 are very similar to the case of fixed contact points, as illustrated in Fig.5, with the secondary vortex system forming at the cavity bottom for large enough depth of the liquid. The surface pressure distributions shown in Fig.6 demonstrate analogous similarities, with the local pressure minima forming above the vortex centres. While the interface recedes below its isothermal location in the cavity centre for the whole range of bulge factors considered, the evolution of the deformation pattern suggests that the interface may rise in the middle of the cavity for larger values of D, in analogy to the case of fixed contact points constraint. The variations of the maximum deformation as a function of Ca are illustrated in Fig.7 and demonstrate the existence of the limit points. An increase of the mass of the liquid from D=-0.5 to D=0 increases Ca_{cr} by a factor of three, but further increase to D=0.5 increases Ca_{cr} only by ap-

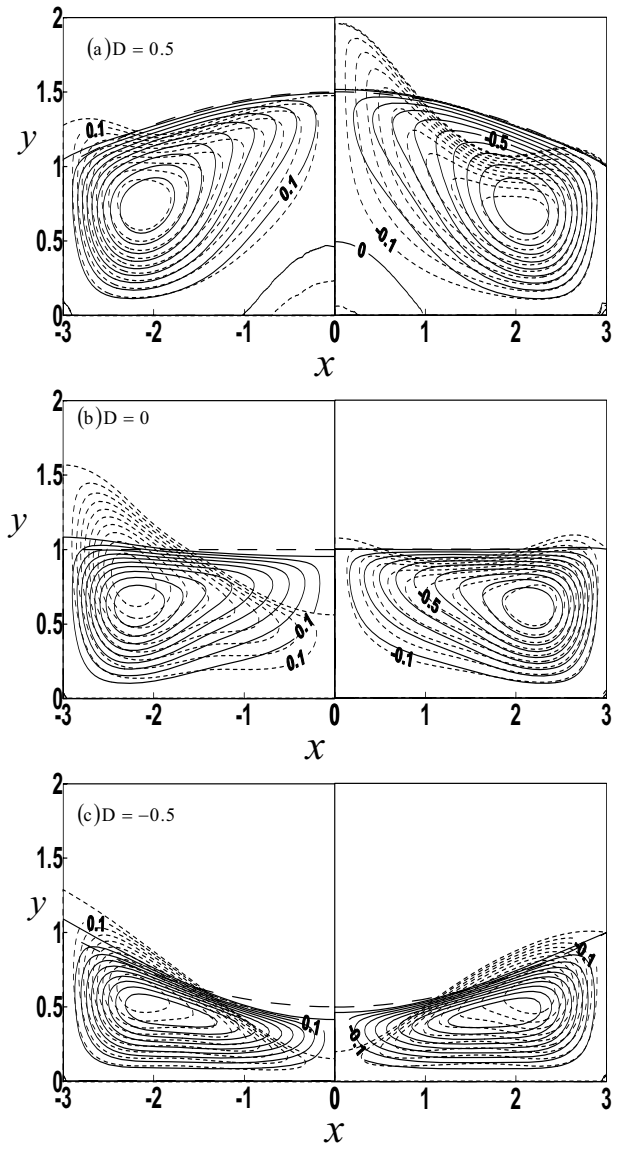

Figure 5 : Flow patterns in a cavity for Re=200; the interface subject to the fixed contact angles constraint (left side) and the fixed contact points constraint (right side). Contour lines are shown every 10% of ψ_{max}. Long-dash lines show isothermal interface. Figure 5a – D=0.5, left side: solid lines - Ca=0.02, —ψ_{max}—=0.1258; dash lines – Ca=0.09, —ψ_{max}—=0.1162; right side: solid lines - Ca=0.02, —ψ_{max}—=0.1245; dash lines – Ca=0.12, —ψ_{max}—=0.0966. Figure 5b – D=0, left side: solid lines - Ca=0.02, —ψ_{max}—=0.0969; dash lines – Ca=0.08, —ψ_{max}—=0.0966; right side: solid lines - Ca=0.02, —ψ_{max}—=0.0963; dash lines – Ca=0.12, —ψ_{max}—=0.0906. Figure 5c – D=-0.5, left side: solid lines - Ca=0.01, —ψ_{max}—=0.0481; dash lines – Ca=0.025, —ψ_{max}—=0.0472; right side: solid lines - Ca=0.01, —ψ_{max}—=0.0514; dash lines – Ca=0.05, —ψ_{max}—=0.0594.

proximately 20%.

4 Conclusions

Investigations of the effects of cavity over-filling and under-filling on the form of thermocapillary convection and interface rupture have been carried out. A simple model problem consisting of a rectangular cavity open from above has been used in the analysis. The cavity is subjected to concentrated heating applied at the liquid interface. The resulting steady-state flow and deformation patterns are determined numerically by solving the com-

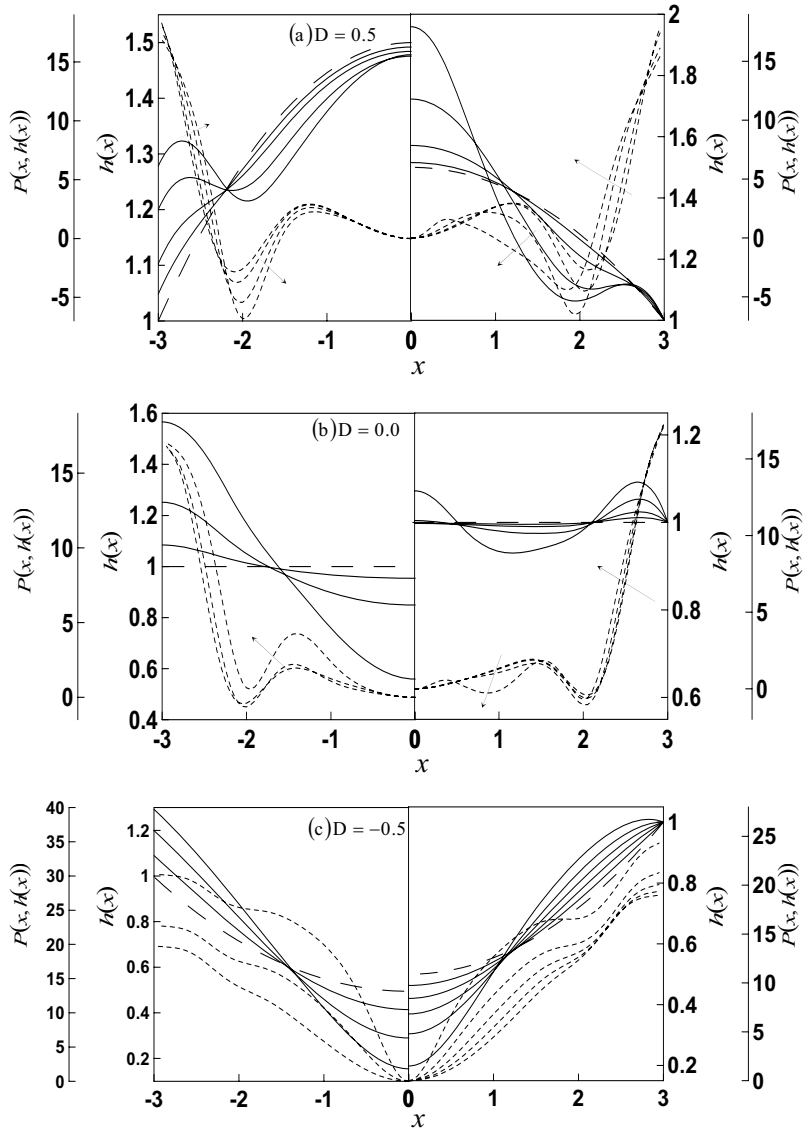

Figure 6 : The evolution of the surface pressure (dash lines) and the shape of the interface (solid lines) as a function of the capillary number Ca for L=6, Re=200; interface subject to the fixed contact angles constraint (left side) and the fixed contact points constraint (right side). The long-dash lines show isothermal interface, solid lines show deformed interface and dash lines show surface pressure. Figure 6a – D=0.5, left side: interface and pressure shown for Ca= 0.02, 0.04, 0.07, 0.09; right side: interface and pressure shown for Ca= 0.02, 0.06, 0.1, 0.12. Figure 6b – D=0, left side: interface and pressure shown for Ca=0.02, 0.05, 0.08; right side: interface and pressure shown for Ca=0.02, 0.04, 0.08, 0.12. Figure 6c –D=-0.5, left side: interface and pressure shown for Ca= 0.01, 0.02, 0.025; right side: interface and pressure shown for Ca=0.01, 0.02, 0.03, 0.04, 0.05. The top dash line always corresponds to the pressure with the smallest Ca unless arrow points out otherwise (arrow directed towards increasing Ca).

plete governing equations including the complete deformation effects. The initial form of the contact conditions is maintained during the heating. Two cases of contact conditions are considered. In the first one, the contact points are fixed during the heating, and in the second one the contact angles are fixed and the liquid is permitted to move along the sidewalls. Detailed results are presented for Ma=0, Bi=∞, L=6.

The results show that steady convection and continuous interface exist only for a certain range of capillary num-

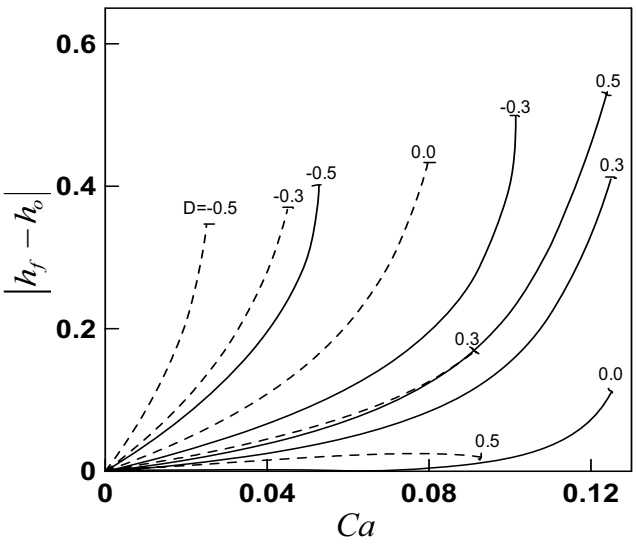

Figure 7 : The interface deformation in the middle of the cavity as a function of the capillary number Ca for different values of the bulge factor D and for Re=200. Continuous and dash lines describe the fixed contact points and the fixed contact angles cases, respectively.

bers Ca. When Ca approaches its critical value, Ca=Ca_{cr} (limit point), the magnitude of the deformation increases rapidly. The shape of the interface implies initiation of a process leading to interface rupture, with the form of potential rupture changing significantly depending on the interface contact conditions.

It is demonstrated that the system response depends on the value of Re and interface contact conditions. For small values of Re, an increase of the mass of the liquid always extends the range of acceptable parameters. When Re is large, increase of the mass of the liquid from D=-0.5 to D=0 increases Ca_{cr}, but further increase permits the "inviscid vortex" effect to dominate and, as a result, Ca_{cr} does not change. When fixed contact angles are replaced by fixed contact points, change of D from D=-0.5 to D=0 increases Ca_{cr} by a factor of three, but further change of D to D=0.5 increases Ca_{cr} by only 20%.

If the rupture presents a concern in a given application, the present results suggests that at first one should attempt to fix the location of the end points of the interface, and then consider adding liquid to the cavity. Some caution must be exercised in the latter case if Re is high enough.

Acknowledgement: This work was supported by the NSERC of Canada. Computing resources have been provided by SHARCNET.

References

Amberg, G.; Shiomi, J. (2005) : Thermocapillary flow and phase change in some widespread materials processes. *FDMP: Fluid Dynamics & Materials Processing*, vol 1, pp. 81-95.

Berdnikov, V.S., Gaponov, V.A., and Kovrizhnykh, L.S. (2001): Thermal gravitational-capillary convection in a cavity with a longitudinal temperature gradient *J. Engineering Phys. & Thermophysics*, vol.74, pp.999-1006.

Chen, J.C. and Hwu, F.S. (1993): Oscillatory thermocapillary flow in a rectangular cavity *Int. J. Heat Mass Transfer*, vol.36, pp.3743-3749.

Chen, C., and Floryan, J.M. (1994): Numerical simulation of non-isothermal capillary interfaces *J. Comp. Phys*., vol.111, pp.183-193.

Chen, J.J., and Lin, J.D. (2000): Thermocapillary effect on drying of a polymer solution under non-uniform radiant heating *Int.J.Heat & Mass Transfer*, vol.43, pp.2155-2165.

Czechowski, L. and Floryan, J.M. (2001): Marangoni instability in a finite container – transition between short and long wavelengths modes *ASME J. Heat Transfer*, vol.23, pp.96-104.

Davis, S.H. (1987): Thermocapillary Instabilities *Ann.Rev.Fluid Mech.*, vol.19, pp.403-435.

El-Gammal, M., Furmanski, P., and Floryan, J.M. (2003): Thermocapillary convection in the over-filled and partially filled cavities *Phys.Fluids*, vol.16, pp.212-215.

Feonychev, A.I. (1995): Comparative analysis of thermocapillary convection in one- and two-layer systems. Problem of oscillatory convection *Adv.Space Res*., vol.16, pp.59-65.

Floryan, J.M. and Chen, C. (1994): Thermocapillary convection and existence of continuous liquid layers in the absence of gravity, *J. Fluid Mech.*, vol.277, pp.303-329.

Gelfgat A.Yu., Rubinov A., Bar-Yoseph P.Z. and Solan A., (2005), "On the Three-Dimensional Instability of Thermocapillary Convection in Arbitrarily Heated Floating Zones in Microgravity Environment" , *FDMP:*

Fluid Dynamics & Materials Processing, Vol. 1, no.1, pp. 21-32

Hamed, M. and Floryan, J.M. (1998): Numerical simulation of unsteady nonisothermal capillary interfaces *J.Comp.Phys*.,vol.145, pp.110-140.

Hamed, M. and Floryan, J.M. (2000a): Marangoni convection. Part 1. A cavity with differentially heated sidewalls *J.Fluid Mech*., vol.405, pp.79-110.

Hamed, M. and Floryan, J.M. (2000b): Marangoni convection. Part 2. A cavity subject to point heating *J.Fluid Mech*., vol.405, pp.111-129.

Herrero, H., and Mancho, A.M. (1998): Influence of aspect ratio in convection due to non-uniform heating *Phys.Rev.E*, vol.52, pp.7336-7339.

Higuera, F.J. (2000): Steady thermocapillary-buoyant flow in an unbounded liquid layer heated non-uniformly from above, *Phys.Fluids,* vol.12, pp.2186-2197.

Jiang, Y., Badr, H., and Floryan, J.M. (2003): Thermocapillary convection with moving contact points *Phys.Fluids*, vol.15, pp.442-454.

Jiang, Y., and Floryan, J.M. (2003): Effect of heat transfer at the interface on the thermocapillary convection in the adjacent phase *ASME J. Heat Transfer*, vol.125, pp.190-194.

Kuhlmann, H.C. (1999): Thermocapillary convection in models of crystal growth *Springer Tracts in Modern Physics*, Springer Berlin Heidelberg, vol.152.

Lappa, M. (2005): On the nature and structure of possible three-dimensional steady flows in closed and open parallelepipedic and cubical containers under different heating conditions and driving forces. *FDMP: Fluid Dynamics & Materials Processing*, vol 1, no 1, pp. 1-19.

Lappa M. **(2005b)**: Review: Possible strategies for the control and stabilization of Marangoni flow in laterally heated floating zones, *FDMP: Fluid Dynamics & Materials Processing*, vol.1, no.2, pp. 171-188.

Lee, K.J., Kamotani, Y., and Yoda, S. (2002): Combined thermocapillary and natural convection in rectangular containers with localized heating *Int.J.Heat and Mass Transfer*, vol.45, pp.4621-4630.

Nepomnyashchy, A.A., and Simanovskii, I.B. (1999): Combined action of different mechanisms of convective instability in multiplayer systems *Phys.Rev.E.*, vol.59, pp.6672-6686.

Pearson, J.R.A.(1958): On convection cells induced by surface tension *J.Fluid Mech*., vol.4, pp.489-500.

Pumir. A, and Blumenfeld, L. (1996): Heat transport in a liquid layer locally heated on its free surface *Phys.Rev.E*, vol.54, pp.R4528-4531.

Rivas, D. (1991): High Reynolds number flows in shallow enclosures *Phys. Fluids A*, vol.3, pp.280-291.

Schatz, M.F. and Neitzel, G.P. (2001): Experiments in Thermocapillary Instabilities *Ann.Rev.Fluid Mech.*, vol.33, pp. 93-127.

Scriven, L.E. and Sterling, C.V. (1960): The Marangoni effect *Nature*, vol.187, pp.186-188.

Simanovskii, I.B. (2000): Combined action of anticonvective and thermocapillary mechanisms of instability in multiplayer systems *Eur.J.Mech.B – Fluids*, vol.19, pp.123-137.

Tan, M.J., Bankoff, S.G., and Davis, S.H. (1990): Steady thermocapillary flows of thin liquid layers. I. Theory *Phys Fluids A*, vol.2, pp.313-321.